Chemical Science

ROYAL SOCIETY OF CHEMISTRY

EDGE ARTICLE

View Article Online
View Journal | View Issue

Cite this: *Chem. Sci.*, 2025, **16**, 20021

All publication charges for this article have been paid for by the Royal Society of Chemistry

Received 4th September 2025
Accepted 22nd September 2025

DOI: 10.1039/d5sc06841j

rsc.li/chemical-science

Enantioselective synthesis of C–C and C–N axially chiral pyrazole-based heterobiaryls

Jun He, Zun Yang, Lili Lin * and Xiaoming Feng *

Axially chiral five-membered heteroaryls are prevalent in bioactive molecules. Their catalytic asymmetric synthesis remains challenging due to their relatively low rotational energy barriers. We developed a chiral nickel(II) complex-catalyzed asymmetric cycloaddition/oxidation sequential reaction of hydrazonoyl chlorides with α,β-unsaturated enones, which involves asymmetric [3 + 2] 1,3-dipolar cycloaddition of hydrazonoyl chlorides with α,β-unsaturated enones followed by oxidation to realize central-to-axial chirality transfer. A class of pyrazole-based heterobiaryls were prepared efficiently with high yields and good enantioselectivities. Based on the mechanistic study and control experiments, a possible mechanism was proposed to elucidate the reaction process and enantioinduction.

Introduction

Atropisomers are widely spread in natural products,[1] drug molecules,[2] materials science,[3] and asymmetric catalysis.[4] Consequently, the catalytic enantioselective synthesis of atropisomers has emerged as a prominent research hotspot within the domain of asymmetric synthesis.[5] Among the diverse classes of atropisomers, six-membered axially chiral (hetero) biaryls, linked *via* C–C axes, represent the most prevalent and well-established structural scaffolds.[6] In contrast, the catalytic asymmetric construction of axially chiral five-membered (hetero)biaryls is relatively less developed (Scheme 1a).[7] This research gap primarily stems from the inherent characteristics of five-membered systems, their lower rotational barriers and diminished configurational stability, which collectively hinder effective stereocontrol during synthesis.[8] In recent years, significant progress has been made in addressing this challenge, with the successful catalytic asymmetric synthesis of axially chiral five–six-membered heterocyclic frameworks, such as aryltriazoles,[9] arylimidazoles,[10] arylisothiazoles,[11] arylfurans,[12] and arylpyrroles.[13] Despite this advancement, the catalytic asymmetric construction of five–five-membered heteroaromatic skeletons remains comparatively underreported; existing studies also tend to focus narrowly on systems with C–C or N–N axes.[14] To the best of our knowledge, only a limited number of reports have thus far described the catalytic asymmetric synthesis of C–N axially chiral five–five-membered heteroaromatic scaffolds.[9e,12f,15]

Arylpyrazole derivatives, representing a class of five-membered heteroaryl atropisomers, are frequently encountered

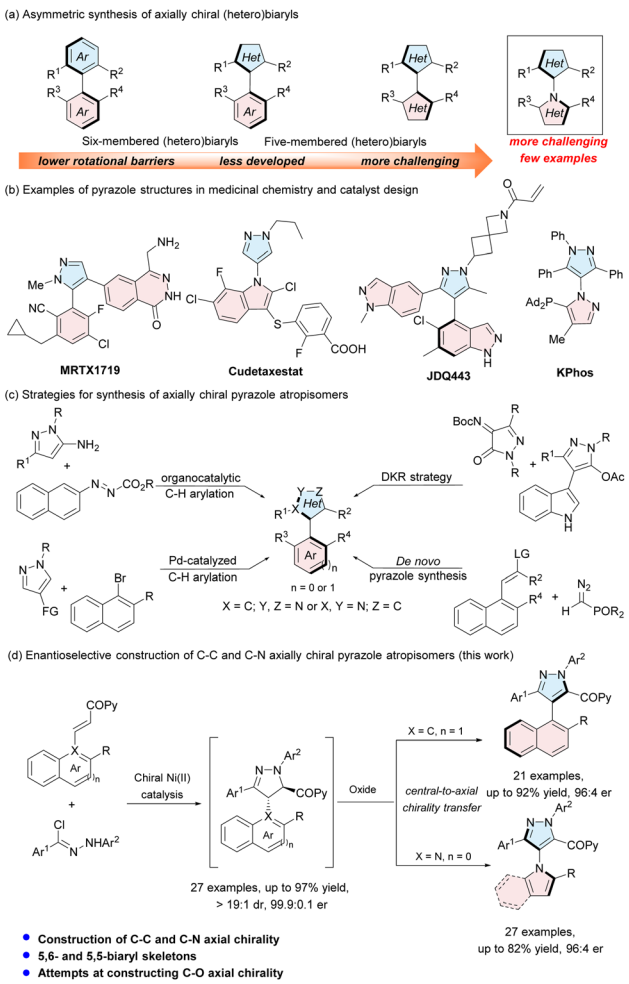

Scheme 1 Background of synthesis of axially chiral pyrazoles.

Key Laboratory of Green Chemistry & Technology, Ministry of Education, College of Chemistry, Sichuan University, Chengdu 610064, P. R. China. E-mail: lililin@scu.edu.cn; xmfeng@scu.edu.cn

in natural products, biologically active compounds and chiral ligands (Scheme 1b).[16] For the synthesis of axially chiral arylpyrazoles, the Li group,[17a] the Tang group[17b] and others,[17c–h] developed an organocatalytic and Pd-catalyzed C–H arylation strategy. Recently, Huang and coworkers have successfully constructed pyrazole-indole scaffolds featuring both C–C axial chirality and central chirality, utilizing a dynamic kinetic resolution (DKR) strategy.[17i] In 2023, the Wang group synthesized axially chiral arylpyrazole atropisomers containing a phosphorus unit through a *De novo* pyrazole synthesis *via* the Huisgen-cycloaddition/aromatization cascade reaction (Scheme 1c).[17j] Despite these notable advances, the development of five–five-membered pyrazole-based heterobiaryls with a C–N chiral axis remains unreported.

Arylhydrazonoyl chlorides are well-documented as 1,3-dipole species and serve as effective precursors for dihydropyrazole synthesis.[18] We hypothesized that reacting sterically hindered aryl-substituted unsaturated ketones with arylhydrazonoyl chlorides in the presence of a chiral Lewis acid would trigger an asymmetric 1,3-dipolar cycloaddition. This reaction would yield centrally chiral dihydropyrazoles, which could then undergo oxidation to form axially chiral arylpyrazoles *via* a central-to-axial chirality transfer process.[19] This strategy would thereby provide a novel approach for the synthesis of axially chiral pyrazole derivatives.

Herein, we report a chiral *N*,*N*′-dioxide/Ni(II) complex-catalyzed asymmetric [3 + 2] cycloaddition/oxidation sequential reaction,[20] which enables the versatile and efficient construction of two distinct classes of axially chiral arylpyrazole atropisomers: C–C-linked five–six-membered systems and C–N-linked five–five-membered systems (Scheme 1d).

Results and discussion

To construct five–six-membered C–C axially chiral arylpyrazole atropisomers, hydrazonoyl chloride **A1** and α,β-unsaturated enone **B1** were selected as model substrates to optimize the reaction conditions *via* a one-pot protocol consisting of [3 + 2] cycloaddition followed by DDQ (2,3-dichloro-5,6-dicyano-1,4-benzoquinone) oxidation (Table 1). Initially, various metal salts were screened by complexing with *N*,*N*′-dioxide **L$_3$-PrPr$_2$**. Most metal salts showed no chiral induction ability, with the exception of Mg(OTf)$_2$, Co(OTf)$_2$, and Ni(OTf)$_2$ though enantioselectivity remained low. The Ni(OTf)$_2$ complex afforded the target axially chiral pyrazole product **C1** in 40% yield with 64 : 36 er (entry 3). Subsequently, the chiral backbone of the ligand was evaluated. (*S*)-Pipecolic acid-derived **L$_3$-PiEt$_2$** proved superior to L-proline-derived **L$_3$-PrEt$_2$** and L-ramipril-derived **L$_3$-RaEt$_2$** in terms of enantioselectivity (entries 4–6). Further investigations into the ligand's amide moiety revealed that 2,6-diethyl-4-adamantyl benzenamine derived **L$_3$-PiEt$_2$Ad** gave **C1** in 23% yield with 77 : 23 er (entry 8). Replacing Et$_3$N with ^{i}Pr$_2$NEt as the base resulted in a slight improvement in both yield and enantiomeric ratio (entry 9). When THF was used as the solvent and the temperature was increased to 40 °C, arylpyrazole product **C1** was obtained in 74% yield with 91.5 : 8.5 er (entry 10). Increasing the loadings of **B1** and ^{i}Pr$_2$NEt, combined with performing the oxidation in EtOAc at 10 °C, further enhanced enantioselectivity while preserving yield (entry 11). Notably, adding a trace amount of H$_2$O as an additive boosted the yield. **C1** was finally produced in 91% yield with 95.5 : 4.5 er (entry 12).

Table 1 Optimization of the reaction conditions[a]

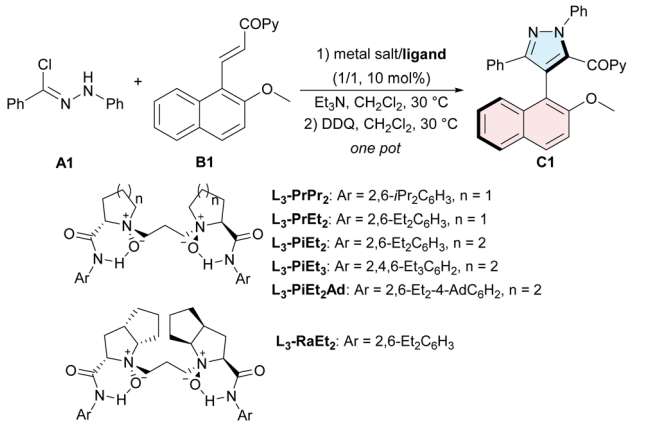

Entry	Metal salt	Ligand	Yield[b] (%)	er[c]
1	Mg(OTf)$_2$	**L$_3$-PrPr$_2$**	23	53.5 : 46.5
2	Co(OTf)$_2$	**L$_3$-PrPr$_2$**	17	57.5 : 42.5
3	Ni(OTf)$_2$	**L$_3$-PrPr$_2$**	40	64 : 36
4	Ni(OTf)$_2$	**L$_3$-PrEt$_2$**	42	64 : 36
5	Ni(OTf)$_2$	**L$_3$-RaEt$_2$**	41	70.5 : 29.5
6	Ni(OTf)$_2$	**L$_3$-PiEt$_2$**	32	73.5 : 26.5
7	Ni(OTf)$_2$	**L$_3$-PiEt$_3$**	27	75.5 : 24.5
8	Ni(OTf)$_2$	**L$_3$-PiEt$_2$Ad**	23	77 : 23
9[d]	Ni(OTf)$_2$	**L$_3$-PiEt$_2$Ad**	26	78 : 22
10[d,e]	Ni(OTf)$_2$	**L$_3$-PiEt$_2$Ad**	74	91.5 : 8.5
11[d,e,f]	Ni(OTf)$_2$	**L$_3$-PiEt$_2$Ad**	78	96 : 4
12[d,e,f,g]	Ni(OTf)$_2$	**L$_3$-PiEt$_2$Ad**	91	95.5 : 4.5

[a] Unless otherwise noted, all reactions were carried out with **A1** (0.1 mmol), **B1** (0.1 mmol), metal/ligand (1/1, 10 mol%), Et$_3$N (0.1 mmol) in DCM (1.0 mL) at 30 °C for 24 h under N$_2$ protection. Subsequently, DDQ (0.1 mmol) and CH$_2$Cl$_2$ (0.5 mL) were added, and the reaction mixture was stirred at 30 °C for 3 h. [b] Isolated yield. [c] Determined by HPLC analysis. [d] ^{i}Pr$_2$NEt (0.1 mmol). [e] THF (0.5 mL) at 40 °C. [f] **A1** (0.14 mmol), ^{i}Pr$_2$NEt (0.14 mmol); EtOAc (1.0 mL) at 10 °C for oxidation. [g] With 3 μL H$_2$O.

With the optimized reaction conditions established, the substrate scope was investigated (Scheme 2). For hydrazonoyl chlorides, substituting the nitrogen-bonded phenyl group with a *p*-bromophenyl or *p*-methoxyphenyl group resulted in lower enantioselectivity (products **C1–C3**). In contrast, using a *p*-trifluoromethylphenyl substituent led to a sharp decline in oxidation reactivity—highlighting the critical role of the nitrogen-bonded substituent in the oxidation step (see the SI for details). Both electron-donating and electron-withdrawing substituents on the aromatic ring of hydrazonoyl chlorides were well-tolerated, affording products **C4–C9** with enantioselectivities ranging from 78.5 : 21.5 er to 88 : 12 er (**C4–C9**). Additionally, naphthaldehyde-derived hydrazonyl chloride was compatible with the reaction, yielding the corresponding axially chiral product **C10** in 85% yield with 88 : 12 er. Next, the scope of α,β-unsaturated enones **B** was explored. Various 2-alkoxy

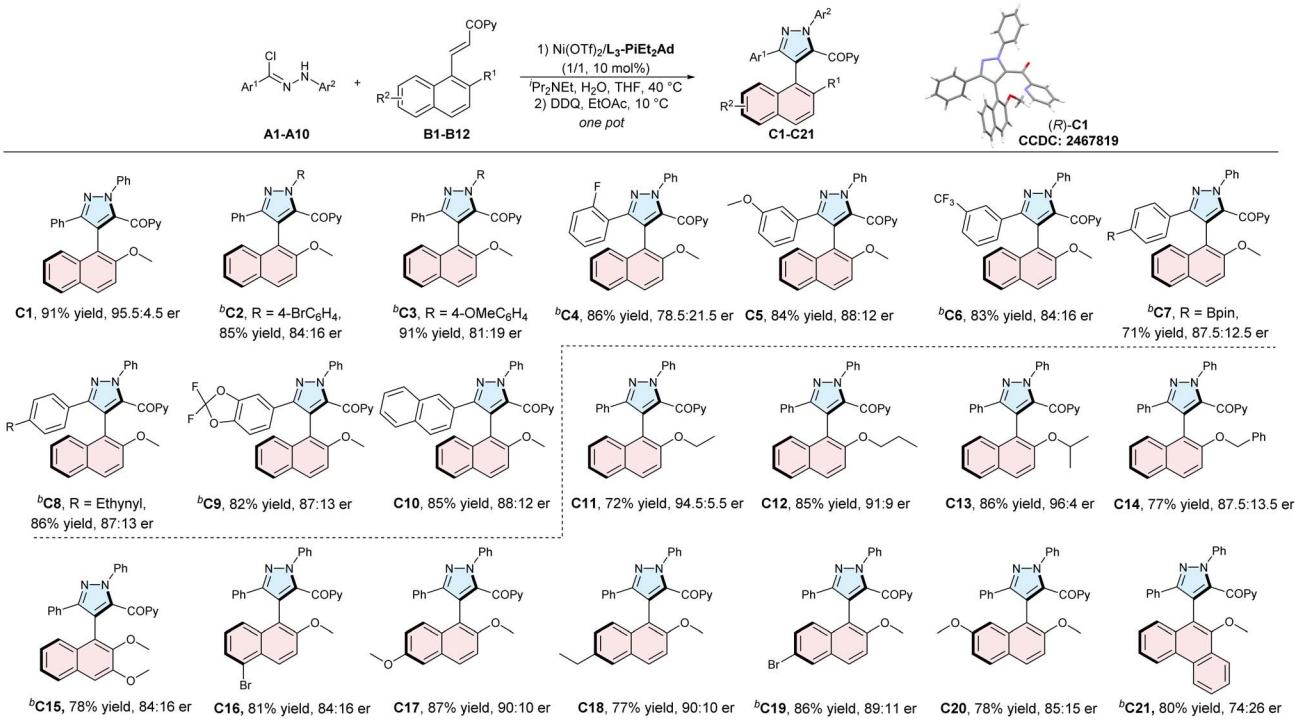

Scheme 2 The substrate scope of C–C axially chiral pyrazoles. [a]Unless otherwise noted, all reactions were carried out with **A** (1.4 equiv.), **B** (0.1 mmol), Ni(OTf)$_2$/**L$_3$-PiEt$_2$Ad** (1/1, 10 mol%), ^{i}Pr$_2$NEt (1.4 equiv.), H$_2$O (3 μL) in THF (0.5 mL) at 40 °C for 24 h under N$_2$ protection. The mixture was subsequently concentrated *in vacuo*. Then, DDQ (1.0 eq.) and EtOAc (1.0 mL) were added, and the reaction mixture was stirred at 10 °C. [b]H$_2$O (4 μL).

substituents were tolerated in the cyclization/oxidation sequence, furnishing target axially chiral products **C11–C14** in high yields and good enantioselectivities. Substitution on the 3, 5, 6, or 7-position of the enone scaffold had little effect on the reaction. Notably, when a phenanthryl-substituted enone **B12** was employed, enantioselectivity decreased sharply (**C21**, 74 : 26 er), which might be due to the increased steric hindrance. The absolute configuration of the product **C1** was determined to be (*R*) *via* single-crystal X-ray diffraction analysis.[21]

Next, α,β-unsaturated enone **D2** was employed to access five–five-membered C–N axially chiral pyrazoles (Table 2). The one-pot protocols led to challenges in purifying product **F2**, as deeply colored impurities were generated. Thus, the cycloaddition product **E2** was isolated prior to the oxidation step. Initially, K_2CO_3 was used as the base; while the diastereomeric ratio (dr) and enantiomeric ratio (er) of the desired product **E2** were excellent (>19 : 1 dr, 99.5 : 0.5 er), the yield was only 43%. Modifying the reaction conditions—switching the solvent from THF to DCM and lowering the temperature from 40 °C to 20 °C—improved the yield of **E2** to 92%, with dr and enantiomeric excess (ee) remaining excellent. Subsequently, the dehydrogenative aromatization of pyrazoline to pyrazole was evaluated. Using DDQ alone as the oxidant led to the slow formation of **F2**, affording the product **F2** in 43% yield with 70 : 30 er (entry 1). Notably, the oxidizing capacity of DDQ is significantly enhanced upon visible light excitation;[22] leveraging this property, the oxidation of **E2** was efficiently achieved using DDQ under blue light irradiation at 20 °C (entry 2). Further accelerating the reaction rate by introducing basic conditions allowed isolation of **F2** in 84% yield with 92 : 8 er. Finally, decreasing the temperature to −20 °C and increasing the reaction basicity further improved the enantiomeric ratio to 95 : 5 (entry 4).

Table 2 Optimization of the reaction conditions for construction of C–N axially chiral pyrazoles[a]

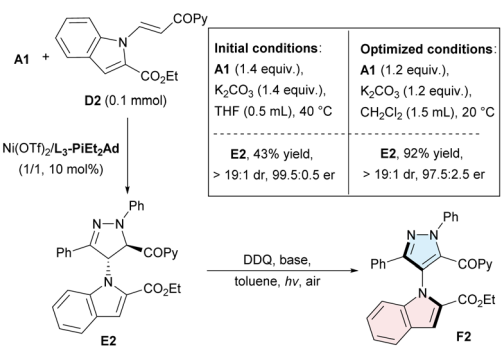

Entry[a]	*hv* (nm)	Base	Yield[b] (%)	er[c]
1[d]	—	—	43	70 : 30
2	420	—	55	70 : 30
3	420	K_2CO_3 (0.8 equiv.)	84	92 : 8
4[e]	420	Cs_2CO_3 (1.0 equiv.)	80	95 : 5

[a] Unless otherwise noted, all oxidations were performed with **E2**, base (1.0 equiv.), DDQ (1.5 equiv.) in toluene (0.1 M) under an air atmosphere at 20 °C and under 5 W LED irradiation. [b] The overall isolated yield of the two steps. [c] Determined by HPLC analysis on a chiral stationary phase. [d] At 60 °C. [e] At −20 °C.

Subsequently, the scope of C–N axially chiral pyrazoles was explored (Scheme 3). For enones with an indolyl tether, modifying the ester group—from methyl to ethyl, isopropyl, or phenyl—had little impact on the reaction performance; cycloaddition products **E1–E4** were obtained in 80–92% yield with > 19 : 1 dr and 96:4–97.5 : 2.5 er, while the corresponding oxidized pyrazoles **F1–F4** were isolated in 67–82% yield with 95 : 5 er. In contrast, replacing the ester group with a benzenesulfonyl group led to reduced enantioselectivity (**E5** and **F5**). When using enone **D6** derived from 2-phenylindole, the cycloaddition product **E6** was formed in high yield and enantioselectivity; however, the subsequent oxidation afforded axially chiral product **F6** with only 80 : 20 er. A wide range of aryl-substituted hydrazonyl chlorides were also evaluated. Those bearing electron-withdrawing or electron-donating groups were well-tolerated in the sequential cycloaddition/oxidation process, with the exception of *p*-ethynyl-substituted derivatives. Specifically, cycloaddition products **E7–E19** were obtained in 80–96% yields with 9 : 1–19 : 1 dr and 82.5 : 17.5–99.9 : 0.1 er, while the oxidized pyrazoles **F7–F19** were isolated in 40–81% yields with 78.5 : 21.5–96 : 4 er. Notably, enones with substituted indole rings, regardless of the electronic properties and positions of the substituents, were compatible with the reaction, furnishing target axially chiral pyrazoles **F20-F26** in 56–82% yields with 93.5 : 6.5–95 : 5 er. A limitation emerged, however, when using the enone **D14** bearing a pyrrole ring, while the cycloaddition product **E27** was formed in 97% yield, it decomposed during oxidation, resulting in only 35% yield of **F27**. Finally, the absolute configurations of **E2** and **F2** were determined *via* single-crystal X-ray diffraction analysis as (4*S*,5*R*) and (*S*),[23] respectively.

Axially chiral diaryl ethers constitute a class of atropisomers characterized by a unique dual C–O axis.[24] Their catalytic enantioselective synthesis currently relies predominantly on

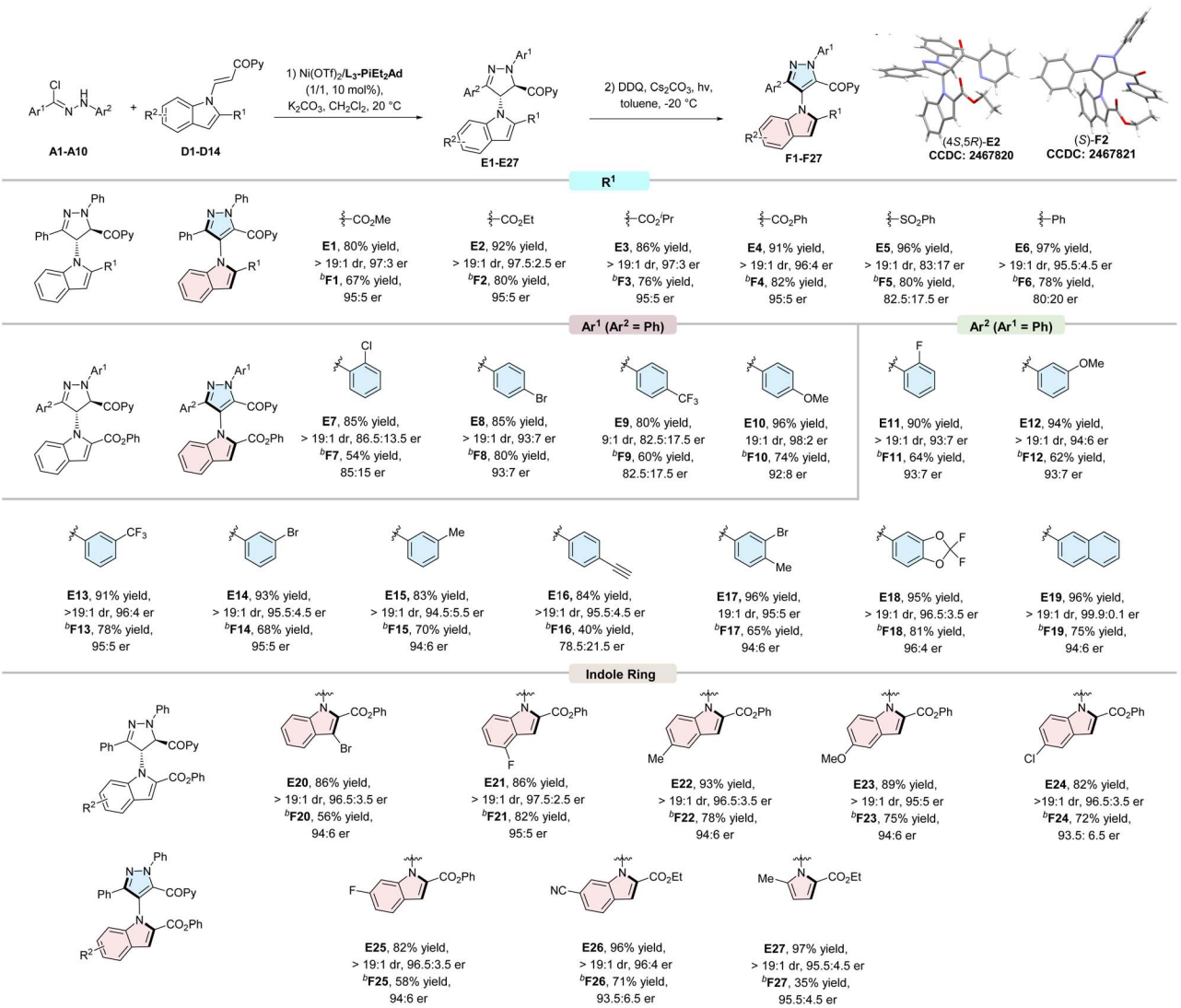

Scheme 3 The substrate scope of C–N axially chiral pyrazoles. [a]Unless otherwise noted, all reactions were carried out with **A** (1.2 equiv.), **D** (0.1 mmol), Ni(OTf)$_2$/**L$_3$-PiEt$_2$Ad** (1/1, 10 mol%), and K_2CO_3 (1.2 equiv.) in CH_2Cl_2 (1.5 mL) at 20 °C for 12 h under N_2 protection. Then, after purification on silica gel, **E**, Cs_2CO_3 (1.0 eq. of **E**), and DDQ (1.5 eq. of **E**) in toluene (0.1 M) were reacted under an air atmosphere at −20 °C and under 5 W 420 nm LED irradiation. [b]The overall isolated yield of the two steps.

desymmetrization strategies. Furthermore, axially chiral diaryl ethers incorporating a five-membered heterocyclic framework remain unreported. Building on our current system, we therefore attempted the synthesis of C–O axially chiral pyrazole derivatives (Scheme 4a). Using $Ni(NTf_2)_2$/**L_3-TQMe$_2$CPh$_3$** as the catalyst, the asymmetric synthesis of compound **E28** was achieved with a 50% NMR yield, >19 : 1 dr and 96 : 4 er.

Subsequent dehydrogenation of **E28** in the presence of *N*-chlorosuccinimide afforded the corresponding C–O axially chiral pyrazole **F28** in 30% yield and 64 : 36 er, which might be attributed to the phenoxy group's robust leaving ability coupled with the conformational flexibility imparted by the two C–O bonds throughout the rearomatization process.

To evaluate the synthetic potential of this protocol, scale-up experiments were conducted. Specifically, hydrazonoyl chloride **A1** was reacted with α,β-unsaturated enone **B1** (3.0 mmol) or **D4** (2.0 mmol), affording the target axially chiral pyrazole **C1** in 83% yield with 94.5 : 5.5 er and **F4** in 64% yield with 94 : 6 er, respectively (Scheme 4b). Subsequently, derivatization studies were performed to expand the synthetic scope. Treatment of **C1** with $NaBH_4$ yielded secondary alcohol **G1** in 89% yield with 1.5 : 1 dr and 93.5 : 6.5 er/93 : 7 er. Additionally, compound **F4** underwent slow chlorination to form product **G2** in 65% yield with 93 : 7 er. To investigate the configurational stability of these axially chiral arylpyrazoles, racemization experiments were carried out to determine the rotational barriers (see the SI for details). For compound **C1**, the free energy of activation ($\Delta G^{\ddagger}$) was calculated to be 27.32 kcal mol^{-1} by monitoring the enantiomeric excess (ee) values at different time intervals at 70 °C. Similarly, the racemization barrier of **F4** was measured to be 29.66 kcal mol^{-1} at 85 °C. The racemization half-life ($t_{1/2}$) of both compounds was also determined. At their respective test temperatures, the $t_{1/2}$ of compound **C1** was calculated to be 3.6 hours, while that of **F4** was calculated to be 16.6 hours.

To gain insight into the mechanism of central-to-axial chirality transfer for C–N axially chiral pyrazoles, control experiments were performed (Scheme 5a). Under either nitrogen or oxygen atmospheres, oxidation of **E4** resulted in significant decreases in both yield and enantioselectivity of product **F4**, indicating that an air atmosphere is critical for the oxidation step. Notably, adding a trace amount of water under an oxygen atmosphere afforded **F4** in 69% yield with 92 : 8 er, suggesting that trace water present in air may act as a promoter. Oxidation conducted under an air atmosphere without DDQ still yielded **F4** in 52% yield, implying that both DDQ and atmospheric oxygen function as oxidants. Additionally, the reaction proceeded under an air atmosphere in the absence of Cs_2CO_3, ruling out a mechanism involving deprotonation of **E4** followed by reaction with oxygen to form a peroxide.[18c] UV-vis absorption spectra revealed that the dearomatized cycloaddition intermediates **E1** and **E4** absorb blue light at 420 nm, whereas their oxidized products **F1** and **F4** exhibit very weak absorption at this wavelength (Scheme 5b). This observation suggests that the cycloaddition intermediates may undergo photoexcitation under light irradiation. In the singlet oxygen trap experiment (Scheme 5c), the addition of singlet oxygen scavengers DHN and DPBF increased the yield of product **F25**, and no products from the reaction of DHN and DPBF with

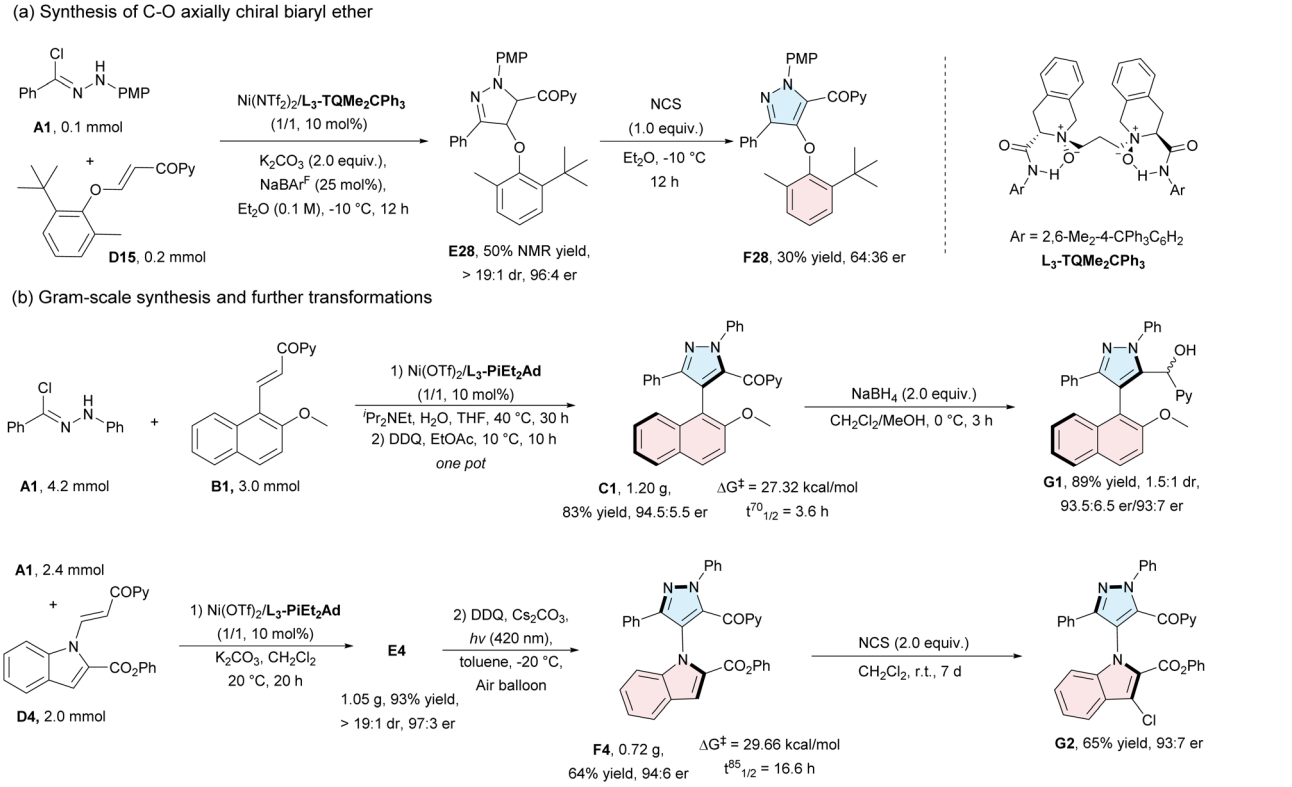

Scheme 4 Gram-scale synthesis and further transformations.

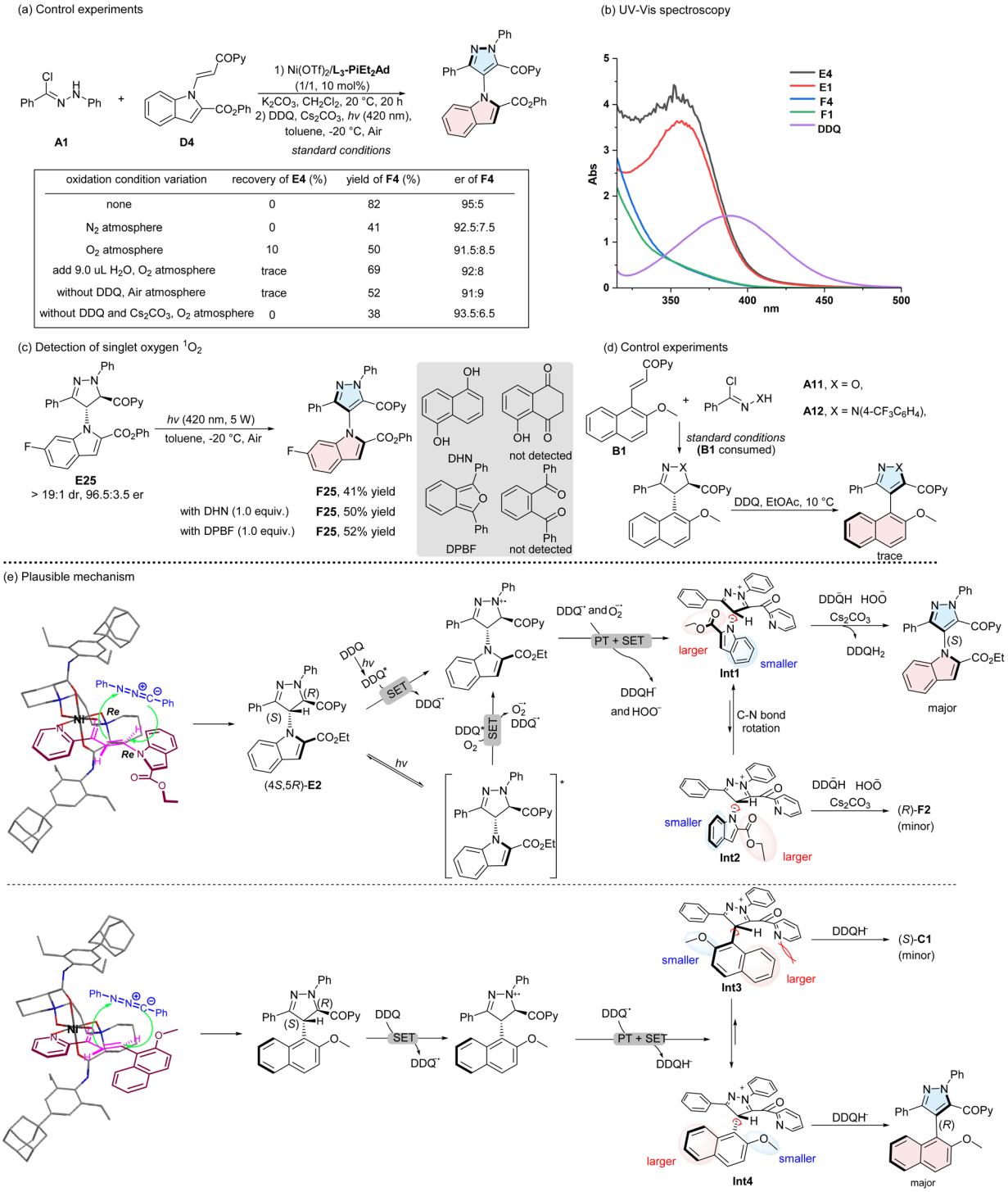

Scheme 5 Mechanistic studies and the proposed mechanism.

singlet oxygen were detected during the reaction process. This indicates that singlet oxygen was not generated upon light irradiation; instead, triplet oxygen reacted directly with photo-excited **E25**. When **A11** was used as the substrate, the oxidation proceeded very slowly, resulting in only trace yields of the corresponding axially chiral product (Scheme 5d). These observations suggest that the DDQ-mediated dehydrogenative rearomatization of dihydropyrazoles proceeds *via* a single-electron transfer (SET) mechanism rather than a direct hydrogen atom transfer (HAT) pathway.

Based on the experimental results and previous studies,[20g,j] a plausible mechanism is proposed in Scheme 5e. The chiral *N*,*N*′-dioxide ligand coordinates to the Ni^{II} center in a tetradentate fashion, forming an octahedral complex. Substrate **D2**

then coordinates bidentately to this *N*,*N*′-dioxide-Ni^{II} catalyst, undergoing cycloaddition with the nitrile imine, predominantly *via* the Re–Re face of **D2**, to form (4*S*,5*R*)-**E2**. Under blue light irradiation, two pathways for oxidation are feasible: (1) **E2** undergoes single-electron oxidation by photoexcited DDQ* to generate a radical cation intermediate and DDQ$^{\cdot-}$; (2) photoexcited **E2** participates in single-electron transfer with oxygen and DDQ*, producing the radical cation intermediate, $O_2^{\cdot-}$ and DDQ$^{\cdot-}$. This radical cation is subsequently converted to a cation *via* proton abstraction mediated by DDQ$^{\cdot-}$ and superoxide $O_2^{\cdot-}$ coupled with a single-electron-transfer step. In this cation intermediate, the *N*-indole group rotates around the C–N bond, generating two rotamers **Int1** and **Int2**. Due to steric repulsion between the larger ester group and other substituents on the dihydropyrazole ring, less sterically hindered **Int1** undergoes efficient central-to-axial chirality transfer, selectively forming (*S*)-**F2**. In contrast, for the C–C axially chiral product **C1**, the naphthyl group exhibits greater steric hindrance than the methoxy group. This drives the reaction to proceed preferentially *via* the less hindered rotamer **Int4**, ultimately affording the (*R*)-**C1** product. The longer C–C bond increases the conformational flexibility in the cationic intermediate, which may account for the lower enantioselectivities compared to the C–N system.

Conclusions

In conclusion, an efficient catalytic asymmetric [3 + 2] cycloaddition/oxidation sequential reaction between hydrazonoyl chlorides and α,β-unsaturated enones was achieved, using a chiral *N*,*N*′-dioxide/Ni(II) complex as the catalyst. This protocol leverages readily accessible starting materials and provides facile access to two distinct classes of axially chiral arylpyrazoles, the C–C five–six-membered and C–N five–five-membered arylpyrazoles, in high yields and good enantioselectivities. The synthetic utility of this methodology is further supported by scale-up experiments, product derivatization studies, and initial attempts to construct the more challenging C–O axially chiral pyrazole scaffolds. Ongoing work is focused on extending this strategy to the enantioselective synthesis of other classes of atropisomers.

Author contributions

J. H. performed experiments and prepared the SI and paper. Y. Z. repeated some experiments. L. L. L. helped with modifying the paper and SI. X. M. F. conceived and directed the project.

Conflicts of interest

There are no conflicts to declare.

Data availability

Further details of the experimental procedure, ^{1}H, ^{13}C{^{1}H} and ^{19}F {^{1}H} NMR spectra, HPLC chromatograms, and X-ray crystallographic data for **C1**, **E2**, **F2** and **D5** are available in the SI. See DOI: https://doi.org/10.1039/d5sc06841j.

CCDC 2467819, 2467820 and 2467821 contain the supplementary crystallographic data for this paper.[21,23,25]

Acknowledgements

The authors acknowledge financial support from the National Key R&D Program of China (2023YFA1506700) and the National Natural Science Foundation of China (No. 22171189). We are grateful to Dr Yuqiao Zhou (Sichuan University) for the X-ray single crystal diffraction analysis.

Notes and references

1 (*a*) J. E. Smyth, N. M. Butler and P. A. Keller, *Nat. Prod. Rep.*, 2015, **32**, 1562–1583; (*b*) G. Bringmann, T. Gulder, T. A. M. Gulder and M. Breuning, *Chem. Rev.*, 2011, **111**, 563–639; (*c*) G. Bringmann, J. Mutanyatta-Comar, M. Knauer and B. M. Abegaz, *Nat. Prod. Rep.*, 2008, **25**, 696–718.

2 (*a*) S. R. Laplante, L. D. Fader, K. R. Fandrick, D. R. Fandrick, O. Hucke, R. Kemper, S. P. F. Miller and P. J. Edwards, *J. Med. Chem.*, 2011, **54**, 7005–7022; (*b*) J. Clayden, W. J. Moran, P. J. Edwards and S. R. LaPlante, *Angew. Chem., Int. Ed.*, 2009, **48**, 6398–6401; (*c*) S. R. LaPlante, P. J. Edwards, L. D. Fader, A. Jakalian and O. Hucke, *ChemMedChem*, 2011, **6**, 505–513; (*d*) Z. Wang, L. Meng, X. Liu, L. Zhang, Z. Yu and G. Wu, *Eur. J. Med. Chem.*, 2022, **243**, 114700; (*e*) S. T. Toenjes and J. L. Gustafson, *Future Med. Chem.*, 2018, **10**, 409–422; (*f*) S. Perreault, J. Chandrasekhar and L. Patel, *Acc. Chem. Res.*, 2022, **55**, 2581–2593.

3 (*a*) L. Pu, *Chem. Rev.*, 1998, **98**, 2405–2494; (*b*) G. A. Hembury, V. V. Borovkov and Y. Inoue, *Chem. Rev.*, 2008, **108**, 1–73.

4 (*a*) Y. Chen, S. Yekta and A. K. Yudin, *Chem. Rev.*, 2003, **103**, 3155–3212; (*b*) T. Akiyama, *Chem. Rev.*, 2007, **107**, 5744–5758; (*c*) W. Tang and X. Zhang, *Chem. Rev.*, 2003, **103**, 3029–3070; (*d*) D. Parmar, E. Sugiono, S. Raja and M. Rueping, *Chem. Rev.*, 2014, **114**, 9047–9153; (*e*) M. P. Carroll and P. J. Guiry, *Chem. Soc. Rev.*, 2014, **43**, 819–833; (*f*) W. Fu and W. Tang, *ACS Catal.*, 2016, **6**, 4814–4858; (*g*) T. Akiyama and K. Mori, *Chem. Rev.*, 2015, **115**, 9277–9306.

5 (*a*) J. K. Cheng, S.-H. Xiang, S. Li, L. Ye and B. Tan, *Chem. Rev.*, 2021, **121**, 4805–4902; (*b*) H.-H. Zhang, T.-Z. Li, S.-J. Liu and F. Shi, *Angew. Chem., Int. Ed.*, 2024, **63**, e202311053; (*c*) H.-H. Zhang and F. Shi, *Acc. Chem. Res.*, 2022, **55**, 2562–2580; (*d*) E. Kumarasamy, R. Raghunathan, M. P. Sibi and J. Sivaguru, *Chem. Rev.*, 2015, **115**, 11239–11300; (*e*) G.-J. Mei, W. L. Koay, C.-Y. Guan and Y. Lu, *Chem*, 2022, **8**, 1855–1893; (*f*) W. Qin, Y. Liu and H. Yan, *Acc. Chem. Res.*, 2022, **55**, 2780–2795; (*g*) A. Gaucherand, E. Yen-Pon, A. Domain, A. Bourhis, J. Rodriguez and D. Bonne, *Chem. Soc. Rev.*, 2024, **53**, 11165–11206; (*h*) S.-H. Xiang, W.-Y. Ding, Y.-B. Wang and B. Tan, *Nat. Catal.*, 2024, **7**, 483–498; (*i*) T. A. Schmidt, V. Hutskalova and C. Sparr, *Nat. Rev. Chem.*, 2024, **8**, 497–517; (*j*) D. Liang,

W. Xiao, S. Lakhdar and J. Chen, *Green Synth. Catal.*, 2022, **3**, 212–218.

6 (*a*) J. Wencel-Delord, A. Panossian, F. R. Leroux and F. Colobert, *Chem. Soc. Rev.*, 2015, **44**, 3418–3430; (*b*) S. Perveen, G. Zhang and P. Li, *Org. Biomol. Chem.*, 2025, **23**, 4006–4023; (*c*) G. Wang, J. Huang, J. Zhang and Z. Fu, *Org. Chem. Front.*, 2022, **9**, 4507–4521; (*d*) R. Song, Y. Xie, Z. Jin and Y. R. Chi, *Angew. Chem., Int. Ed.*, 2021, **60**, 26026–26037; (*e*) P. Loxq, E. Manoury, R. Poli, E. Deydier and A. Labande, *Coord. Chem. Rev.*, 2016, **308**, 131–190; (*f*) J. A. Carmona, C. Rodríguez-Franco, R. Fernández, V. Hornillos and J. M. Lassaletta, *Chem. Soc. Rev.*, 2021, **50**, 2968–2983; (*g*) X. Zhang, Y.-Z. Liu, H. Shao and X. Ma, *Molecules*, 2022, **27**, 8517; (*h*) O. Quinonero, M. Jean, N. Vanthuyne, C. Roussel, D. Bonne, T. Constantieux, C. Bressy, X. Bugaut and J. Rodriguez, *Angew. Chem., Int. Ed.*, 2016, **55**, 1401–1405; (*i*) L. E. Zetzsche, J. A. Yazarians, S. Chakrabarty, M. E. Hinze, L. A. M. Murray, A. L. Lukowski, L. A. Joyce and A. R. H. Narayan, *Nature*, 2022, **603**, 79–85.

7 (*a*) T. Z. Li, S. J. Liu, W. Tan and F. Shi, *Chem.–Eur. J.*, 2020, **26**, 15779–15792; (*b*) D. Bonne and J. Rodriguez, *Eur. J. Org Chem.*, 2018, **2018**, 2417–2431; (*c*) D. Bonne and J. Rodriguez, *Chem. Commun.*, 2017, **53**, 12385–12393; (*d*) Y.-C. Zhang, F. Jiang and F. Shi, *Acc. Chem. Res.*, 2020, **53**, 425–446; (*e*) W. Luo, Y. Zhang, M. Ming and L. Zhang, *Org. Chem. Front.*, 2024, **11**, 6819–6849.

8 (*a*) X.-L. He, C. Wang, Y.-W. Wen, Z. Wang and S. Qian, *ChemCatChem*, 2021, **13**, 3547–3564; (*b*) S. Zhang, G. Liao and B. Shi, *Chin. J. Org. Chem.*, 2019, **39**, 1522–1528; (*c*) I. Alkorta, J. Elguero, C. Roussel, N. Vanthuyne and P. Piras, *Advances in Heterocyclic Chemistry*, Elsevier, 2012, vol. 105, pp. 1–188.

9 (*a*) X. Zhang, S. Li, W. Yu, Y. Xie, C.-H. Tung and Z. Xu, *J. Am. Chem. Soc.*, 2022, **144**, 6200–6207; (*b*) W.-T. Guo, B.-H. Zhu, Y. Chen, J. Yang, P.-C. Qian, C. Deng, L.-W. Ye and L. Li, *J. Am. Chem. Soc.*, 2022, **144**, 6981–6991; (*c*) L. Zeng, J. Li and S. Cui, *Angew. Chem., Int. Ed.*, 2022, **61**, e202205037; (*d*) L. Zeng, F. Zhang and S. Cui, *Org. Lett.*, 2023, **25**, 443–448; (*e*) L. Zhou, Y. Li, S. Li, Z. Shi, X. Zhang, C.-H. Tung and Z. Xu, *Chem. Sci.*, 2023, **14**, 5182–5187; (*f*) S. Choi, M. C. Guo, G. M. Coombs and S. J. Miller, *J. Org. Chem.*, 2023, **88**, 7815–7820.

10 (*a*) Y. Kwon, A. J. Chinn, B. Kim and S. J. Miller, *Angew. Chem., Int. Ed.*, 2018, **57**, 6251–6255; (*b*) Y. Kwon, J. Li, J. P. Reid, J. M. Crawford, R. Jacob, M. S. Sigman, F. D. Toste and S. J. Miller, *J. Am. Chem. Soc.*, 2019, **141**, 6698–6705; (*c*) N. Man, Z. Lou, Y. Li, H. Yang, Y. Zhao and H. Fu, *Org. Lett.*, 2020, **22**, 6382–6387; (*d*) P. Zhang, X.-M. Wang, Q. Xu, C.-Q. Guo, P. Wang, C.-J. Lu and R.-R. Liu, *Angew. Chem., Int. Ed.*, 2021, **60**, 21718–21722; (*e*) F.-B. Ge, Q.-K. Yin, C.-J. Lu, X. Xuan, J. Feng and R.-R. Liu, *Chin. J. Chem.*, 2024, **42**, 711–718; (*f*) Q.-J. An, W. Xia, W.-Y. Ding, H.-H. Liu, S.-H. Xiang, Y.-B. Wang, G. Zhong and B. Tan, *Angew. Chem., Int. Ed.*, 2021, **60**, 24888–24893; (*g*) L. Hou, S. Zhang, J. Ma, H. Wang, T. Jin, M. Terada and M. Bao, *Org. Lett.*, 2023, **25**, 5481–5485; (*h*) Z.-J. Zhang, M. M. Simon, S. Yu, S.-W. Li, X. Chen, S. Cattani, X. Hong and L. Ackermann, *J. Am. Chem. Soc.*, 2024, **146**, 9172–9180; (*i*) S. Yin, J. Liu, K. N. Weeks and A. Aponick, *J. Am. Chem. Soc.*, 2023, **145**, 28176–28183.

11 (*a*) Y. Chang, C. Xie, H. Liu, S. Huang, P. Wang, W. Qin and H. Yan, *Nat. Commun.*, 2022, **13**, 1933; (*b*) Y. Yan, M. Li, Q. Shi, M. Huang, W. Li, L. Cao and X. Zhang, *Asian J. Org. Chem.*, 2023, **12**, e202200578; (*c*) Y. Chen, T. Wang, Z. Wang and C. Zhu, *Chem*, 2025, **11**, 102592.

12 (*a*) V. S. Raut, M. Jean, N. Vanthuyne, C. Roussel, T. Constantieux, C. Bressy, X. Bugaut, D. Bonne and J. Rodriguez, *J. Am. Chem. Soc.*, 2017, **139**, 2140–2143; (*b*) J.-Y. Wang, C.-H. Gao, C. Ma, X.-Y. Wu, S.-F. Ni, W. Tan and F. Shi, *Angew. Chem., Int. Ed.*, 2024, **63**, e202316454; (*c*) S. Zhang, Q.-J. Yao, G. Liao, X. Li, H. Li, H.-M. Chen, X. Hong and B.-F. Shi, *ACS Catal.*, 2019, **9**, 1956–1961; (*d*) S. Qiu, X. Gao and S. Zhu, *Chem. Sci.*, 2021, **12**, 13730–13736; (*e*) X. Bao, J. Rodriguez and D. Bonne, *Chem. Sci.*, 2020, **11**, 403–408; (*f*) Y.-Q. Guan, K.-G. Ma, D.-C. Wang and H.-M. Guo, *Org. Lett.*, 2025, **27**, 5094–5100.

13 (*a*) Y.-B. Chen, Y.-N. Yang, X.-Z. Huo, L.-W. Ye and B. Zhou, *Sci. China Chem.*, 2023, **66**, 2480–2491; (*b*) J. Feng, C.-J. Lu and R.-R. Liu, *Acc. Chem. Res.*, 2023, **56**, 2537–2554.

14 (*a*) X.-M. Wang, P. Zhang, Q. Xu, C.-Q. Guo, D.-B. Zhang, C.-J. Lu and R.-R. Liu, *J. Am. Chem. Soc.*, 2021, **143**, 15005–15010; (*b*) P. Zhang, Q. Xu, X.-M. Wang, J. Feng, C.-J. Lu, Y. Li and R.-R. Liu, *Angew. Chem., Int. Ed.*, 2022, **61**, e202212101; (*c*) W. Yao, C.-J. Lu, L.-W. Zhan, Y. Wu, J. Feng and R.-R. Liu, *Angew. Chem., Int. Ed.*, 2023, **62**, e202218871; (*d*) Q. Xu, H. Zhang, F.-B. Ge, X.-M. Wang, P. Zhang, C.-J. Lu and R.-R. Liu, *Org. Lett.*, 2022, **24**, 3138–3143; (*e*) X.-L. He, H.-R. Zhao, X. Song, B. Jiang, W. Du and Y.-C. Chen, *ACS Catal.*, 2019, **9**, 4374–4381; (*f*) Z. Peng, P. Huang, A. Li, M. Yang, Z. Li, Y. Li, S. Qin, J. Cai, S. Wang, Z. Zhou, W. Yi, H. Gao and Z. Zeng, *ACS Catal.*, 2025, **15**, 1422–1430; (*g*) M. Tian, D. Bai, G. Zheng, J. Chang and X. Li, *J. Am. Chem. Soc.*, 2019, **141**, 9527–9532; (*h*) J. Feng and R.-R. Liu, *Chem.–Eur. J.*, 2024, **30**, e202303165; (*i*) C. Ma, F. Jiang, F.-T. Sheng, Y. Jiao, G.-J. Mei and F. Shi, *Angew. Chem., Int. Ed.*, 2019, **58**, 3014–3020.

15 (*a*) O. Kitagawa, *Acc. Chem. Res.*, 2021, **54**, 719–730; (*b*) F. Colobert and B.-F. Shi, *Chem Catal.*, 2021, **1**, 483–485; (*c*) Y.-J. Wu, G. Liao and B.-F. Shi, *Green Synth. Catal.*, 2022, **3**, 117–136; (*d*) P. Rodríguez-Salamanca, R. Fernández, V. Hornillos and J. M. Lassaletta, *Chem.–Eur. J.*, 2022, **28**, e202104442; (*e*) Y.-J. Wu, G. Liao and B.-F. Shi, *Green Synth. Catal.*, 2022, **3**, 117–139.

16 (*a*) M. Achmatowicz, T. Scattolin, D. R. Snead, D. J. Paymode, S. Roshandel, C. Xie, G. Chen and C.-Y. Chen, *Org. Process Res. Dev.*, 2023, **27**, 954–971; (*b*) J. Spicer, N. Blais, S. Owen, A. G. Robinson, Q. Chu, C. Labbe, B. Shieh, P. Brown-Walker, J. Sederias, K. Jensen, A. F. Farago, M.-S. Tsao, T. R. Cottrell, B. Kidane, S. Laurie, R. Juergens, P. A. Bradbury, W. Tu and P.-O. Gaudreau, *Clin. Lung Cancer*, 2025, **26**, 146–151; (*c*) D. Ma, Z. Tan, S. Li, B. Zhao, L. Yue, X. Wei, S. Xu, N. Jiang, H. Lei and X. Zhai, *J. Med.*

Chem., 2025, **68**, 792–818; (*d*) K. Choi, J. N. Brunn, K. Borate, R. Kaduskar, C. Lizandara Pueyo, H. Shinde, R. Goetz and J. F. Hartwig, *J. Am. Chem. Soc.*, 2024, **146**, 19414–19424.

17 (*a*) S. Tong, J. Pu, Y. Qi and S.-W. Li, *Org. Lett.*, 2025, **27**, 932–936; (*b*) Z. Liu, B. Gao, K. Chernichenko, H. Yang, S. Lemaire and W. Tang, *Org. Lett.*, 2023, **25**, 7004–7008; (*c*) Q. Nguyen, S. Guo, T. Royal, O. Baudoin and N. Cramer, *J. Am. Chem. Soc.*, 2020, **142**, 2161–2167; (*d*) H. Yuan, Y. Li, H. Zhao, Z. Yang, X. Li and W. Li, *Chem. Commun.*, 2019, **55**, 12715–12718; (*e*) S.-N. Zhao, Q. Li, X.-X. Qiao, Y. He, G. Li and X.-J. Zhao, *Chem.–Eur. J.*, 2024, **30**, e202402843; (*f*) X. Gao, C. Li, L. Chen and X. Li, *Org. Lett.*, 2023, **25**, 7628–7632; (*g*) X. Luo, S. Li, Y. Tian, Y. Tian, L. Gao, Q. Wang and Y. Zheng, *Eur. J. Org Chem.*, 2024, **27**, e202400254; (*h*) J. Liu, X. Wei, Y. Wang, J. Qu and B. Wang, *Org. Biomol. Chem.*, 2024, **22**, 4254–4263; (*i*) C. Li, W.-F. Zuo, J. Zhou, W.-J. Zhou, M. Wang, X. Li, G. Zhan and W. Huang, *Org. Chem. Front.*, 2022, **9**, 1808–1813; (*j*) J.-H. Wu, J.-P. Tan, J.-Y. Zheng, J. He, Z. Song, Z. Su and T. Wang, *Angew. Chem., Int. Ed.*, 2023, **62**, e202215720.

18 (*a*) T. Hashimoto and K. J. Maruoka, *Chem. Rev.*, 2015, **115**, 5366–5412; (*b*) Y.-C. Tian, J.-K. Li, F.-G. Zhang and J.-A. Ma, *Adv. Synth. Catal.*, 2021, **363**, 2093–2097; (*c*) L. Gao, R. Shi, Y. Tian, X. Luo, Y. Zheng and Q. Wang, *ChemistrySelect*, 2021, **6**, 12838–12842; (*d*) W.-J. Luo, X. Liang, M. Chen, K.-H. Wang, D. Huang, J. Wang, D.-P. Chen and Y. Hu, *J. Org. Chem.*, 2024, **89**, 10066–10076.

19 C. Lemaitre, S. Perulli, O. Quinonero, C. Bressy, J. Rodriguez, T. Constantieux, O. G. García Mancheño and X. Bugaut, *Molecules*, 2023, **28**, 3142.

20 (*a*) X. H. Liu, L. L. Lin and X. M. Feng, *Acc. Chem. Res.*, 2011, **44**, 574–587; (*b*) X. H. Liu, H. F. Zheng, Y. Xia, L. L. Lin and X. M. Feng, *Acc. Chem. Res.*, 2017, **50**, 2621–2631; (*c*) M.-Y. Wang and W. Li, *Chin. J. Chem.*, 2021, **39**, 969–984; (*d*) S. X. Dong, X. H. Liu and X. M. Feng, *Acc. Chem. Res.*, 2022, **55**, 415–428; (*e*) D.-F. Chen and L.-Z. Gong, *Org. Chem. Front.*, 2023, **10**, 3676–3683; (*f*) S. X. Dong, W. D. Cao, M. P. Pu, X. H. Liu and X. M. Feng, *CCS Chem.*, 2023, **5**, 2717–2735; (*g*) D. Zhang, S. Z. Su, Q. W. He, Z. K. Wu, Y. Q. Zhou, C. J. Pan, X. H. Liu and X. M. Feng, *J. Am. Chem. Soc.*, 2020, **142**, 15975–15985; (*h*) X. Y. Hu, L. Cheng, H. Y. Li, Q. F. Xu, X. H. Liu and X. M. Feng, *ACS Catal.*, 2023, **13**, 6675–6682; (*i*) K. Q. Hu, D. Zhang, S. Y. Wang, L. L. Lin and X. M. Feng, *Org. Chem. Front.*, 2023, **10**, 2422–2428; (*j*) C. R. Xu, K. X. Wang, D. W. Li, L. L. Lin and X. M. Feng, *Angew. Chem., Int. Ed.*, 2019, **58**, 18438–18442; (*k*) L. L. Lin, Y. Q. Zhou, W. D. Cao, S. X. Dong, X. H. Liu and X. M. Feng, *Sci. Sin. Chem.*, 2023, **53**, 246–258.

21 CCDC 2467819 (**C1**) contains the supplementary crystallographic data for this paper. These data are provided free of charge by the joint Cambridge Crystallographic Data Centre and Fachinformationszentrum Karlsruhe Access Structures service, DOI: **10.5517/ccdc.csd.cc2ntz2k**.

22 (*a*) P. Natarajan and B. König, *Eur. J. Org Chem.*, 2021, **2021**, 2145–2161; (*b*) I. Maclean, E. Gallent, O. Orozco, A. Molina, N. Rodríguez, J. Adrio and J. C. Carretero, *Org. Lett.*, 2024, **26**, 922–927.

23 CCDC 2467820 (**E2**) and CCDC 2467821 (**F2**), DOI: **10.5517/ccdc.csd.cc2ntz3l**.

24 (*a*) A. Naghim, J. Rodriguez, O. Chuzel, G. Chouraqui and D. Bonne, *Angew. Chem., Int. Ed.*, 2024, **63**, e202407767; (*b*) R. Farooqi, A. Mustafai, A. G. Woldegiorgis, X. Lin and P. Wang, *ACS Catal.*, 2025, **15**, 7891–7911.

25 CCDC 2467821: Experimental Crystal Structure Determination, 2025, DOI: **10.5517/ccdc.csd.cc2ntz4m**.